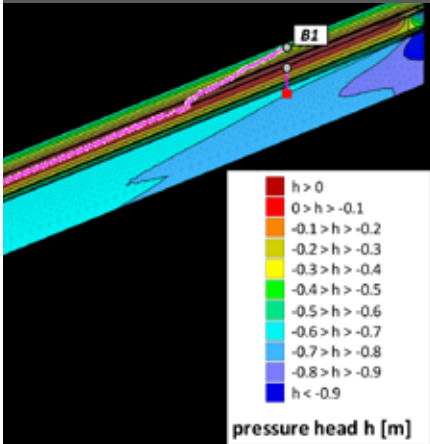


Luisa Hopp*
 Jeffrey J. McDonnell
 Pete Condon



Experience with the performance of soil cover systems over waste rock dumps in cool and humid climates is limited. We measured lateral subsurface flow from a multilayer soil cover system located in Southeast Alaska and used the numerical model HYDRUS-2D to better understand internal flow processes and partitioning of water.

L. Hopp and J.J. McDonnell, Dep. of Forest Engineering, Resources and Management, Oregon State Univ., Corvallis, OR 97331; P. Condon, Hecla Greens Creek Mining Company, P.O. Box 32199, Juneau, AK 99803. *Corresponding author (Luisa.Hopp@oregonstate.edu).

Vadose Zone J. 10
 doi:10.2136/vzj2010.0094
 Received 15 July 2010.
 Published online 19 Jan. 2011.

© Soil Science Society of America
 5585 Guilford Rd., Madison, WI 53711 USA.
 All rights reserved. No part of this periodical may be reproduced or transmitted in any form or by any means, electronic or mechanical, including photocopying, recording, or any information storage and retrieval system, without permission in writing from the publisher.

Lateral Subsurface Flow in a Soil Cover over Waste Rock in a Humid Temperate Environment

The performance of cover systems over waste rock piles in humid, temperate regions (i.e., where annual precipitation > annual potential evapotranspiration) is likely to be defined largely by their ability to shed water laterally within the cover. Lateral flow processes in this context are still poorly understood. Here we present a field and modeling study of the mechanisms that produce lateral subsurface flow and vertical percolation in a 7-yr-old cover system at a mining site in Southeast Alaska. The cover consists of a growth medium on top of a coarse drainage layer, underlain by a highly compacted barrier layer. A second coarse drainage layer separates the cover system from the underlying waste rock. We installed a trench to measure lateral subsurface flow in the cover and then successfully modeled this behavior, without calibration, using a two-dimensional physics-based model. Our results show that the cover responds rapidly to precipitation, converting approximately two-thirds of the input to lateral subsurface flow. Lateral subsurface flow is preceded by the development of transient perched water tables at the interface of the coarse drainage layer and compacted barrier layer. Water balance simulations indicate that flow through the barrier layer is driven by a small but permanent vertical pressure head gradient that develops within the barrier layer and results in vertical net percolation of approximately 15% of the precipitation input. These model results correspond well with lysimeter measurements of vertical percolation into the waste rock.

Abbreviations: AGA, amino G acid monopotassium salt; BL, barrier layer; GM, growth medium; LAI, leaf area index; LCB, lower capillary break layer; pE, potential evaporation; pET, potential evapotranspiration; pT, potential transpiration; RPP, reinforced polypropylene; SCF, surface cover fraction; UCB, upper capillary break layer.

Soil cover systems are employed at waste containment facilities and mining sites as a reclamation strategy. Such systems are intended to isolate waste material from the atmosphere and biosphere, thus protecting environmental resources and public health. In most cases, the primary objective of covers is to minimize net percolation and/or oxygen ingress into the underlying waste material (O’Kane et al., 1998). The individual cover design needs to account for local climatic conditions. In arid and semiarid regions, store-and-release covers (also called evapotranspiration or water balance covers) have often been employed. These systems are designed to retain infiltrating water until it is removed from the soil by evaporation and/or transpiration by employing a storage layer often in combination with a capillary barrier. This type of cover has been widely used in practice and tested extensively (Ward and Gee, 1997; Dwyer, 2003; Albright et al., 2004; Nyhan, 2005; Kelln et al., 2007; McGuire et al., 2009). One-dimensional assessment of water and oxygen flux has usually proved sufficient in such tests because there is little if any lateral flow in the shallow subsurface (Bohnhoff et al., 2009).

In humid and very humid regions, particularly at higher latitudes, water partitioning is different than in arid and semiarid regions, affecting cover design and performance considerably. In these humid and temperate regions store-and-release covers may not be appropriate. Covers in humid and very humid regions and on steeper terrain need to be able to minimize surface runoff (to prevent mass wasting) and to accommodate high water inputs by diverting percolating water laterally downslope in the shallow subsurface to limit water and oxygen ingress into the underlying waste material. Designs are often complex and include a hydrologically resistive barrier, such as a highly compacted fine-grained soil (Yanful et al., 1999). The hydrologic behavior of cover systems in humid and very humid areas that are designed to induce lateral subsurface flow is poorly understood (Ayres et al., 2003). This is because the normal method of assessment of cover performance, regardless of climate regime, comes from lysimeters installed beneath the cover that primarily measure

vertical fluxes (O’Kane et al., 1998; Bews et al., 1999; Simms and Yanful, 1999; Benson et al., 2001). For covers with low-conductivity barrier layers employed in humid temperate regions, the lateral subsurface flow (or interflow) within the cover will likely be a substantial component of the water balance, directly controlling the net percolation into the waste material. In these environments, maximizing lateral flow improves performance.

Recent studies have begun to examine lateral flow directly in cover systems. Kelln et al. (2007, 2009) measured lateral flow in a sloping reclamation cover in the oil sands region of Alberta, Canada, by using a perforated pipe installed in the subsurface at the interface of the cover and underlying shale waste rock. They found that lateral subsurface flow was an important flow process within the cover, mainly generated during snow melt in this cold, semiarid climate. While such studies have helped to identify lateral subsurface flow and internal moisture dynamics in cover systems, the role of lateral subsurface flow for cover performance remains an open question.

Here we present a trench-based study applying techniques borrowed from the field of hillslope hydrology to examine the hydrologic behavior of a soil cover in a region with high rainfall year round. We used a trench excavated at the base of the cover hillslope to capture all water moving laterally from the permeable unconsolidated material above the waste rock. We then parameterized a two-dimensional finite element model (HYDRUS-2D) based on laboratory- and field-measured material properties and tested the model parameterization against the measured lateral flow data for natural rainfall events. We used the model as a learning tool to better understand the lateral subsurface flow dynamics. Thus, the objectives of the paper are to answer the following questions: How is water converted from vertical to lateral flow within the cover? Can a numerical model represent the measured flow partitioning? Are water balance estimates based on measured

lateral subsurface flow and modeling consistent with water balance estimates based on measurements of climatic data and of vertical drainage from a lysimeter? How do lateral flow processes within an engineered cover system compare with lateral flow generation on natural hillslopes?

Materials and Methods

Study Site and Cover Description

The study site is located at the Hecla Greens Creek mine site on Admiralty Island, southeast Alaska (58°04’ N, 134°38’ W). The site is situated in the humid-temperate (oceanic) climatic region, with a mean annual air temperature of 5°C and a mean annual precipitation of 1454 mm (1944–2007, Juneau Airport, National Weather Service, NOAA). Continuous onsite measurements of precipitation from 2001 to 2006 yielded a mean annual rainfall of 1833 mm (see Fig. 1a for location of weather station and rain gauge). Rain events are usually characterized by long duration and low intensities, rarely exceeding 10 mm h⁻¹. The site also receives snow, typically during the months of November to March, and snow covers of 1-m depth are common. Based on onsite measurements of climatic data from 2001 to 2006, annual potential evaporation (Penman, 1948) ranged between 375 and 468 mm (unpublished data, 2001–2006, O’Kane Consultants Inc., Saskatoon, Canada).

The 4047-m² test cover was constructed in 1999 and 2000 and engineered to a 3:1 planar slope (Fig. 1a). It has a south-facing aspect, and the slope has a slight tilt to the southwest. The cover system is designed to convey infiltrating water laterally downslope within the cover and to restrict oxygen and water ingress into the underlying waste rock to a minimum in the long term. It is comprised of four layers and has a total thickness of approximately 1.8 m (Fig. 1b). The growth medium (GM, 0–0.7 m) is uncompacted colluvium and glacial till, with a measured grain size distribution:

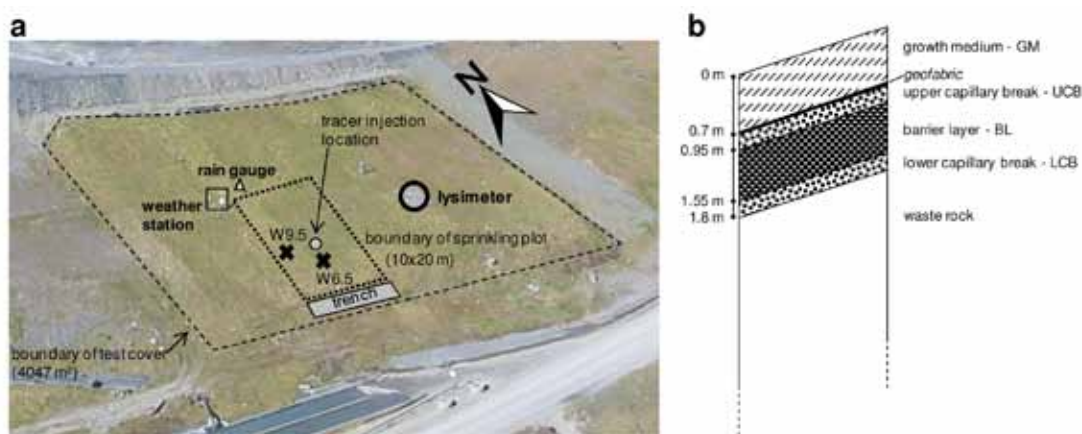


Fig. 1. (a) Aerial photo of test cover showing location of the weather station and rain gauge, the lysimeter and the sprinkling plot including the trench, the two wells and the tracer injection location (not to scale). At the lower end of the photo is the stormwater pond where drainage water from the waste rock site including the test cover is collected and pumped to a treatment plant. (b) Schematic of the cover profile. Depths of layers are below surface. Materials: GM, growth medium (uncompacted colluvium and glacial till); UCB, upper capillary break (coarse gravel); BL, barrier layer (screened, highly compacted till and colluvium); LCB, lower capillary break (same as UCB).

gravel (>4.75 mm) 65.6%, sand (0.075– 4.75 mm) 23.8%, silt and clay (<0.075 mm) 10.6%, and is intended to support vegetation, isolate the barrier layer from freezing conditions, and provide moisture to maintain barrier layer saturation. Below the GM is a 0.25-m-thick upper capillary break layer (UCB) composed largely of coarse gravel (grain diameters 0.5–5 cm) designed to act as a drainage layer. The UCB also minimizes evaporative flux upward from the barrier layer beneath it. A geofabric placed between GM and UCB acts as a filter for vertical movement of fine material. The barrier layer (BL) is 0.6 m thick and consists of a highly compacted mixture of screened till and colluvial material (38.6% gravel, 25.5% sand, 35.9% silt and clay; bulk density $\sim 2.4 \text{ g cm}^{-3}$). The BL is designed to retain a high moisture content (>85% relative saturation) in conjunction with a low hydraulic conductivity to minimize oxygen diffusion and water percolation to the underlying materials. A second (lower) capillary break (LCB, with the same specifications as the UCB) separates the BL from the underlying waste rock (argillite: 76.5% gravel, 19% sand, 4.5% silt and clay). Each layer interface is clear and distinct. The southern edge of the cover is free draining. The lower layers pinch out at the toe and are covered by the GM.

The surface of the cover was seeded with a mix of creeping red fescue (*Festuca rubra* L.), Alta fescue (*Festuca arundinacea* Schreb.), and white Dutch clover (*Trifolium repens* L.) in 2000. The plant cover at the time of our field investigation (7 yr after construction) was well established, with roots uniformly distributed within the GM. The roots formed a dense mat on top of the geofabric, but they were also growing through the geofabric, reaching through the UCB into the first few centimeters of the BL. Volunteer Sitka Spruce [*Picea sitchensis* (Bong.) Carrière] seedlings and moss have also begun to colonize the cover surface. Surface runoff has not been observed on the test cover to date.

As a measure of cover performance, vertical percolation through the cover system into the underlying waste rock has been monitored with a lysimeter that was installed at the time of construction of the cover (Fig. 1a). The lysimeter is a high-density polyethylene cylinder with an inside diameter of 1.5 m and a height of 2.0 m that was inserted into the waste rock layer below the cover. It was backfilled with approximately 1.75

m of compacted waste rock and 0.25 m of UCB material. The lysimeter's upper surface lies just below the bottom of the BL. Water that accumulates in the lysimeter is routed through a sump drain and pipe at the base of the lysimeter to a continuously recording tipping bucket. The performance goal for percolation through the cover was set at "no more than 10% of precipitation" (in agreement with regulatory agencies of the State of Alaska). Monitoring during the past 9 yr since cover construction has shown increasing vertical percolation of up to 19% of precipitation in 2006. The observed exceedance of the performance goal prompted the experiments detailed in this study.

Instrumentation and Experiments

Subsurface Flow Collection System

In May 2007 a trench excavation was performed in the lower southwest corner of the test pad (Fig. 1a). The approximate overall trench length was 10 m. An excavator was used to expose the toe of the slope. The excavation extended to the lower capillary break. Little waste rock (argillite) was exposed during the digging. The exposed trench face was angled for stability purposes. A wooden frame was constructed to increase the stability of the capillary breaks and allow for a support structure for a water collection system. This frame utilized plywood to retain the cobbles in the capillary break. The studs of the frame extended from the bottom of the exposed slope to above the top of the trench face. To increase the stability of the GM, a piece of geofabric was draped over the exposed face and staked into place. Additional sheets of plywood were placed between the GM and the studs. Plastic tarps were placed over the structure to prevent any incident rainfall from landing on the trench face. In November 2007 a 12- by 6-m enclosure was constructed over the trench to protect the trench surface and gutter system. Despite protection from snow and rain, freezing conditions damaged the collection system during the winter. Insulation and a heater were installed in November 2008.

Lateral subsurface flow from each layer was measured directly by a gutter system and continuously recording tipping buckets (Fig. 2). The outflow from the GM was measured in two sections (left and right), each having its own tipping bucket (capacity $\sim 0.1 \text{ L}$). To capture the lateral flow from the GM, the upper portion of the UCB was removed and a length of reinforced polypropylene (RPP) lining

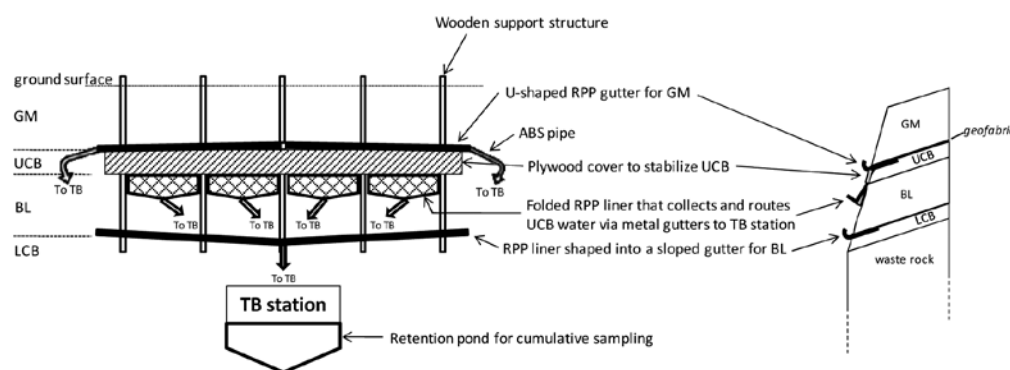


Fig. 2. Illustration of the trench installation in front (left) and side (right) view (not to scale). Materials: GM, growth medium (uncompacted colluvium and glacial till); UCB, upper capillary break (coarse gravel); BL, barrier layer (screened, highly compacted till and colluvium); LCB, lower capillary break (same as UCB); RPP, reinforced polypropylene; TB, tipping bucket. Tarps and other liners that were used to protect the GM are not shown.

material was inserted into this interface (underneath the geofabric). This RPP liner was folded down into the void between the plywood and excavated UCB gravel and back up to the top of the plywood, creating a U-shaped gutter. This RPP gutter was backfilled with UCB material to refill the gap between the plywood and UCB. The liner then drained water to either edge of the face and was routed via an ABS pipe to a tipping bucket. A slightly different approach was taken to capture lateral flow from the UCB layer. This layer was assumed to produce the largest amount of lateral flow. Therefore, the UCB was separated into four gauged sections across the face (UCB-left, UCB-middle left, UCB-middle right, and UCB-right). The RPP liner was fastened to the UCB–BL interface with nails, and the underside of the liner was sealed with bentonite. The liner was then folded to allow water to collect and flow to the tipping buckets (capacity ~ 1 L) via galvanized metal gutters. The BL was expected to produce very limited amounts of lateral flow due to low hydraulic conductivities. An installation technique similar to the GM gutter system was used. However, the layer drained to one central point for the entire exposed face. Liner was inserted at the BL–LCB interface and then shaped into a sloped gutter at the face. It was then filled as a french drain, with a shallow layer of gravels and cobbles, overlain with geofabric and backfilled with BL material. The backfill material was then compacted.

The tipping buckets were centrally located in a RPP liner basin, and the water was routed to a small retention pond. This pond allowed for cumulative sampling and monitoring of water characteristics, such as tracers. The tipping bucket data was recorded using a datalogger (CR-10, Campbell Scientific, Inc., Logan, UT).¹ Calibration of the tipping buckets was performed onsite by passing a known volume of water through each bucket to calculate an average measured volume for each tip.

Installation of Wells

We expected transient perched water tables at the interface between UCB and BL in response to rainfall and snowmelt events. We further expected that any water table development would be short-lived due to the high hydraulic conductivity of the UCB and the hydraulic gradient imposed by the 3:1 planar slope. Two wells were installed on the test cover 6.5 m (W6.5) and 9.5 m (W9.5) upslope of the trench (Fig. 1a). The holes for the wells were bored with a power auger to a depth of approximately 1 m (i.e., boundary between the UCB and the BL) and sealed with silica sand and bentonite. The wells consisted of PVC pipes (5-cm diam.) that were screened for the lowermost 0.2 m. The wells were equipped with water level recorders (Tru Track, New Zealand) with internal dataloggers. The water level recorders were fully functional after May 2007.

Steady-State Sprinkling with Tracer Injection

A steady-state sprinkling experiment was conducted on 16 and 17 May 2007 on a 10- by 20-m plot directly upslope of the trench

to study the hydrologic response of the cover system under controlled conditions. The sprinklers were operated for 15 h with an approximate flow rate of 12 mm h^{-1} . After a 2-h delay, the sprinklers were again turned on for 1 h to bring the cover system back to steady-state outflow. After this 1-h period, the sprinklers were turned off and a tracer was injected into the UCB to estimate mean subsurface flow velocities during drainage. The injection point was 9.5 m upslope of the trench along its centerline. A solution with 120 mg of the fluorescent dye tracer amino G acid monopotassium salt (AGA) was poured down an auger hole. The AGA concentrations were analyzed in samples from the combined discharge in the retention pond (total lateral subsurface flow) using a fluorometer (model 10-AU, Turner Designs, Sunnyvale, CA). Mean lateral subsurface flow velocity was estimated by dividing the distance from the injection point to the trench (9.5 m) by time to peak AGA concentration (Mosley, 1979).

Natural Rainfall Monitoring (Summer 2007)

Significant lateral subsurface flow was recorded when a series of five rain events between 6 and 25 July 2007, produced 145 mm of rainfall. Total lateral subsurface flow, subsurface runoff coefficients (percentage of precipitation returned as lateral subsurface flow), partitioning of the subsurface flow between layers, and lag times between precipitation peaks and discharge peaks were analyzed for the sprinkling experiment as well as for the natural rainfall.

Modeling

Model Domain and Parameterization

We used the finite element model HYDRUS-2D (Simunek et al., 2006) to simulate water flow in the cover system. HYDRUS-2D uses the Richards equation to simulate the movement of water in variably saturated porous media. Since the test cover is planar with no obvious divergence or convergence, we assumed that this system could be adequately described in two dimensions. The slope length of the model domain (46 m) was derived from a detailed digital elevation model based on high-resolution LIDAR data.

We specified parameters where possible based on laboratory and field measurements. Soil water characteristic curves of the GM, BL, and waste rock and saturated hydraulic conductivity (K_s) of the BL and waste rock were determined in the laboratory before construction (G.W. Wilson, personal communication, 1998). Characteristic curves were measured using a modified pressure plate cell described by O’Kane (1996), and K_s was measured using a falling head apparatus (O’Kane, 1996). The K_s for the GM was based on our own field measurements made using hand-augered holes and a constant head permeameter (Ksat, Inc., North Carolina). These measurements were made in three sections of the test cover (downslope, midslope, upslope) and at two depths (0.2–0.3 and 0.4–0.5 m), with up to three replicates. Augering deeper than 0.3 m was difficult due to large rocks and woody debris; this allowed for only three measurements in the depth range of 0.4 to 0.5 m. The side walls of the boreholes were brushed before measurements to reduce

¹ The mention of trade names of commercial products in this paper is for identification purposes only.

the effect of smearing of the walls. The measured K_s values ranged from 0.01 to 0.24 m h⁻¹, with a mean of 0.082 m h⁻¹ and a coefficient of variation of 88%. A trend with slope position or depth was not discernible and the mean K_s value was used for the GM. The K_s value for the UCB and LCB layers was based on the mean UCB subsurface flow velocity that was estimated from the previously described tracer experiment. The van Genuchten–Mualem soil hydraulic model (van Genuchten, 1980) was used to describe the hydraulic properties of the layer materials (Table 1, Fig. 3). Van Genuchten parameters of GM, BL, and waste rock were obtained by fitting the van Genuchten soil hydraulic model to the measured soil water characteristic curves. The soil water characteristics curve of the coarse UCB and LCB material had not been measured; therefore, parameters were based on literature values. The van Genuchten parameters residual water content (θ_r), saturated water content (θ_s), and shape parameter n of the UCB and LCB were specified based on literature values for gravel (Table 1 in Morris and Stormont, 1999). Instead of adopting the value for the shape parameter α used by Morris and Stormont (1999), this parameter was set to 100 m⁻¹ to reflect the small pressure head necessary to induce drainage of the coarse UCB and LCB material and at the same time ensure good mass balances of the simulations (mass balance error < 1%) at the current spatial resolution of the finite element mesh.

Parameters were not adjusted; that is, no calibration was performed. Due to the highly contrasting hydraulic properties of the layers, a very fine spatial discretization of the model domain at layer interfaces with finite element sizes of 0.05 to 0.1 m (Fig. 4) was required to avoid numerical instabilities and to yield good mass balances. The model domain included the four cover layers (total thickness of 1.8 m) plus 2.2 m of the underlying waste rock; the mesh consisted of 27266 nodes and 53918 finite elements.

Table 1. Soil hydraulic parameters of the cover system materials used in the model: θ_r , residual water content; θ_s , saturated water content; α and n , van Genuchten shape parameters; K_s , saturated hydraulic conductivity.

	Thickness	θ_r	θ_s	α	n	K_s
	m			m ⁻¹		m h ⁻¹
Growth medium	0.7	0.08†	0.309†	0.341†	1.177†	0.082‡
Upper and lower capillary break	0.25	0.005§	0.42§	100¶	2.19§	4.2‡
Barrier layer	0.6	0.02†	0.273†	0.112†	1.694†	3.6 × 10 ⁻⁵ †
Waste rock	1.2	0.012†	0.41†	5.43†	2.03†	0.072†

† Based on laboratory measurements before construction (G.W. Wilson, written communication, 1998).
 ‡ Based on field measurements made during this study.
 § Based on values for gravelly materials in Morris and Stormont (1999).
 ¶ Set manually.

We did not represent the geofabric in the model. Studies on the determination of hydraulic properties of geotextiles have shown that hydraulic properties in general resemble very coarse soils, in conjunction with high porosities of more than 80% (Stormont et al., 1997; Iryo and Rowe, 2003; Bouazza et al., 2006; Nahlawi et al., 2007). Research on the unsaturated behavior of geotextiles indicates that they can provide enhanced drainage as well as impede flow, depending on prevailing soil suctions. Due to their hydraulic properties, the hydraulic conductivity of geotextiles drops sharply within a narrow range of soil suctions, with air entry values being typically between 4 and 12 cm of soil suction. Little is known about how the hydraulic properties of geotextiles placed in earthen structures change over time when fines and organic material accumulate in the geotextile, thus decreasing porosity and potentially making the hydraulic properties more similar to finer grained soils. To test if the presence of a geofabric affects lateral subsurface flow we ran a few exploratory water flow simulations on a 3-m segment of the hillslope. Scenarios included without geofabric, with new geofabric, with geofabric treated with fines (hydraulic parameters of the new and treated geofabric were taken from Iryo and Rowe, 2003). No significant differences in lateral subsurface flow were detected between the scenarios, and we therefore decided not to represent

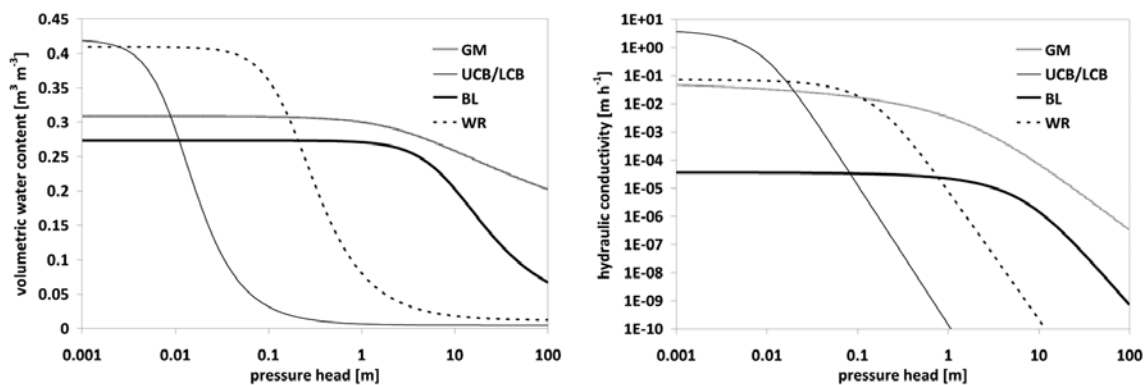


Fig. 3. Soil water characteristic curves and hydraulic conductivity functions of the cover materials used in the model (van Genuchten–Mualem soil hydraulic model). GM, growth medium; UCB/LCB, upper/lower capillary break; BL, barrier layer; WR, waste rock. See Table 1 for function parameters.

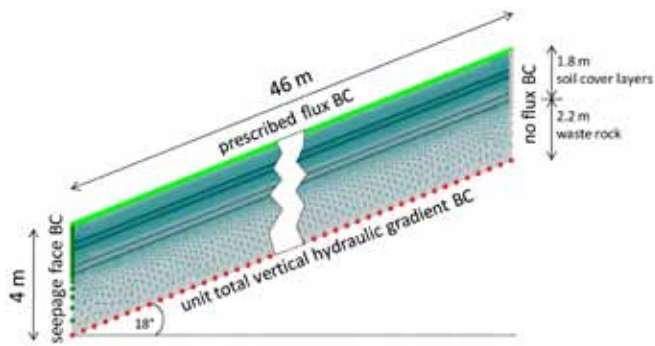


Fig. 4. HYDRUS-2D model domain showing the finite element mesh, dimensions and boundary conditions (BC). Model domain has 27266 nodes and 53918 finite elements. Black lines within the domain separate material layers. The central section of the domain was omitted to more clearly show details of the mesh configuration. Distance between bottom boundary nodes (red squares) is 0.475 m.

the geofabric in the model. The geofabric has a thickness of a few millimeters; its incorporation into the model would require a very fine spatial discretization of the model domain in that area. This would strongly increase the number of finite elements of the mesh with consequences for simulation run times (e.g., the mesh of the 3-m hillslope segment with geofabric had approximately four times as many finite elements as the hillslope segment without geofabric).

Boundary Conditions

At the surface, atmospheric boundary conditions with prescribed fluxes (precipitation and potential evaporation), using hourly climate data from the on-site weather station, were specified (Fig. 4). Also, root water uptake was considered in the simulations. The water stress response function by Feddes et al. (1978) was used, with root water uptake parameters for grass taken from a database included in HYDRUS-2D (for details see User Manual of HYDRUS-2D/3D, for public download at <http://www.pc-progress.com/en/Default.aspx?h3d-downloads> [verified 14 Dec. 2010]). Root water uptake parameters of this model define pressure head ranges with maximum uptake rates (equal to potential transpiration rates) and ranges close to saturation and approaching the wilting point, respectively, with reduced water uptake. We assumed that roots were only present in the growth medium, uniformly distributed throughout the depth of this layer. Potential evapotranspiration rates were estimated with the Penman–Monteith combination equation for reference evapotranspiration (Monteith, 1981; Monteith and Unsworth, 1990) using hourly records of air temperature, relative humidity, wind speed, and net radiation (all measured at the 2-m height). Estimated potential evapotranspiration (pET) was separated into potential evaporation pE (to be applied to the surface boundary of the domain) and potential transpiration pT (to be used in the root water uptake calculations) by using leaf area index (LAI) and surface cover fraction (SCF). The LAI was estimated using the reference crop clipped grass at a height of 0.2 m (Allen et al., 1989). The SCF that indicates the fraction of ground surface covered by vegetation can be computed

from LAI and a radiation extinction coefficient with an exponential equation analogous to Beer's Law (Sinclair, 2006). Multiplication of pET with SCF yields pT and $pET - pT = pE$. HYDRUS calculates the actual evapotranspirative loss based on the availability of water in the soil profile. A seepage face boundary condition was imposed at the downslope end of the hillslope; that is, water leaves the flow domain through the saturated part of the boundary. At the bottom of the domain a free drainage boundary condition was specified, assuming a unit total vertical hydraulic gradient (i.e., a zero pressure head gradient), whereas the upslope boundary was assumed to be no-flux.

Model Testing

For testing the model, we simulated the hydrologic response of the cover system to the July 2007 rain events (145 mm of rainfall) and compared it with our field observations. Initial conditions were obtained from a spin-up simulation that was driven by climate data from the preceding 66 d (1 May–5 July 2007). The final spatial distribution of pressure heads of this spin-up simulation was used as initial condition for the simulation. Total potential evapotranspiration was 30.4 mm, with 89% attributed to potential transpiration. Simulated trench discharge (i.e., lateral subsurface flow leaving the flow domain through the GM, the UCB, and the BL) was divided by the length of the domain (46 m) to facilitate the comparison with field observations. Trench discharge measured in the field was divided by an assumed contributing area of 10 by 46 m. Model performance was evaluated with the Nash–Sutcliffe efficiency statistic (Nash and Sutcliffe, 1970), calculated for the log-transformed values of simulated and observed trench discharge as:

$$NSE = 1 - \frac{\sum_{t=1}^n (\log P_t - \log O_t)^2}{\sum_{t=1}^n (\log O_t - \bar{O})^2}$$

where P_t represents the modeled values, O_t represents the observed values, n is the number of measurements, and \bar{O} is the mean of the observed log-transformed values. The logarithmic transformation leads to a higher sensitivity of the NSE toward low flow conditions, that is, interstorm periods (Krause et al., 2005). The efficiency statistic ranges between 1 and $-\infty$, with 1 indicating a perfect match between observed and modeled values and NSE less than zero indicating that the mean of observations is a better predictor for O_t than the model.

Using the Model to Understand Internal Behavior of the Cover System

A 1-yr simulation based on climate data of 2006 (1822 mm total rainfall and 320 mm estimated potential evapotranspiration with 89% attributed to potential transpiration) was used to establish a water balance of the cover system, to explore the vertical flow through the cover, and to compare results with measurements of water balance components and vertical percolation obtained

from the long-term monitoring of the cover performance. Initial conditions were generated by simulation of hydrologic response driven by observed precipitation and potential evapotranspiration estimates for the duration of 2005. The final pressure head distribution of this spin-up simulation was used as the initial condition for the water balance simulation. Boundary conditions were identical to the model setup described in the previous section. The model output that was used for the calculation of the water balance included the cumulative boundary fluxes (precipitation, actual evapotranspiration, lateral subsurface flow, and flow across the bottom of the BL) and time series of storage in the cover layers. In addition, flowing particles tracing water molecules were released at the beginning of the simulation at two different locations (midslope and upslope) and in two different depths (in the GM near the surface and in the upper few centimeters of the BL). The trajectories of these flowing particles through the cover were followed to assess the fate of infiltrating rain.

Results

Observed Hydrologic Response to Controlled Conditions

Measured lateral subsurface flow commenced 25 min after the onset of the sprinkling, indicating a very short response time of the cover system to incoming rainfall (Fig. 5). Steady-state (constant) outflow at an approximate rate of 8 mm h^{-1} was reached 2.25 h after the start of the sprinkling. Outflow was observed from the UCB and the GM. We noted that outflow from the GM appeared to leave the trench particularly through the geofabric (placed between GM and UCB as a filter for fines), which seemed to provide a preferred flow pathway. The recession started within 30 min after the sprinklers had been turned off. Recession curves were steep, with a half-life of flow of 40 min and a recession index K (time required for flow to recede to 10% of peak flow) of 8.75 h. The subsurface runoff coefficient was 74%, with the UCB contributing 85% and the GM 15% of total flow. If we assumed that up to 19% of infiltrating precipitation drained vertically through the cover (according to lysimeter measurements), then the fraction of input water not recovered was at least approximately 7%. Since the test cover has a slight tilt to the southwest, it seems likely that part of the subsurface flow bypassed the trench on the western side. The high subsurface runoff coefficient may have been at least to some extent attributable to a high relative saturation due to the prolonged irrigation of the cover.

Observed Hydrologic Response to Natural Rainfall

Lateral subsurface flow also occurred under natural conditions (Fig. 6). Lag times between rainfall peaks and discharge peaks were 2 to 6 h, depending on how long the rainless period before the event had been. The lateral subsurface flow showed a “flashy” behavior with distinct responses to individual events, returning quickly to a baseflow-like outflow. Lateral subsurface flow accounted for

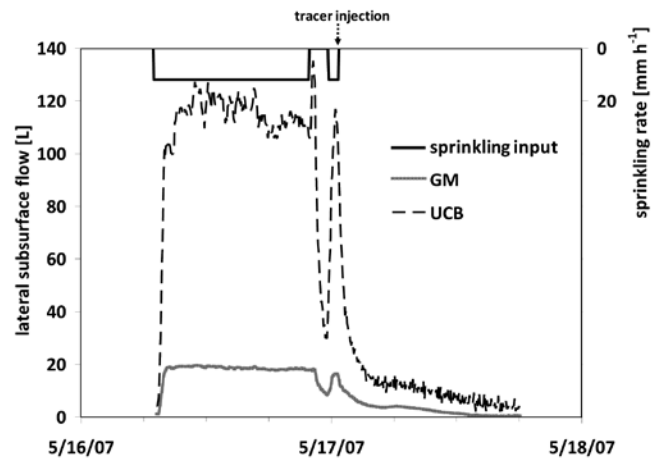


Fig. 5. Lateral subsurface flow collected from growth medium (GM) and upper capillary break (UCB) in response to steady-state sprinkling. Lateral subsurface flow is given in 5 min intervals. Sprinkling rate was approximately 12 mm h^{-1} for 15 h, followed by 2 h of drainage only and 1 h of sprinkling again with the same rate.

approximately 62% of measured precipitation, calculated for the entire period 6 through 25 July 2007. Subsurface runoff coefficients of individual storms varied between 29 and 77%, depending on storm size. Plotting total lateral subsurface flow vs. total event rainfall indicated a linear relationship between the two variables above a certain threshold value for the precipitation (for the observed range of events). This threshold value, which indicates the minimum rainfall necessary for the initiation of significant subsurface lateral flow, was estimated to be around 10 mm (Fig. 7). The partitioning between GM and UCB was similar to observations during the sprinkling, with the UCB contributing approximately 88% and the GM 12% of total flow. The contribution from the GM was mostly during storm periods, and it decreased substantially during interstorm

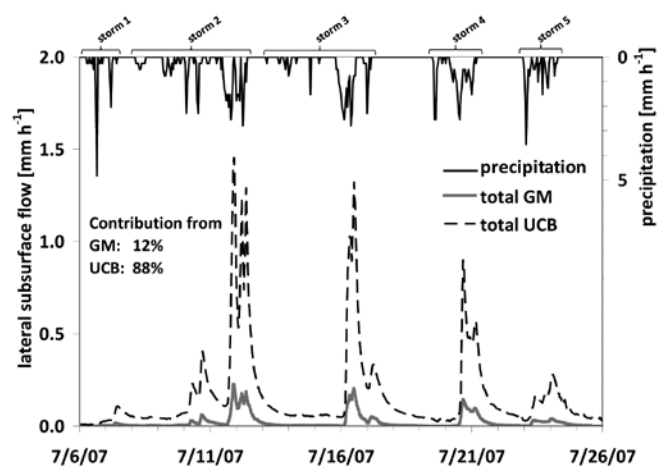


Fig. 6. Lateral subsurface flow collected from growth medium (GM) and upper capillary break (UCB) in response to rainfall events in July 2007. Lateral subsurface flow was normalized by an assumed upslope contributing area of 10 m by 46 m. Total amount of rainfall during the three week period was 145 mm.

periods. Subsurface flow was triggered by transient perched water table development at the UCB–BL interface (Fig. 8). Maximum water table heights recorded in the wells varied with storm size and ranged between 11 and 20 cm; that is, they did not rise into the GM. The two wells exhibited very different response patterns. Well W9.5 showed short-lived water tables, whereas in Well W6.5 water tables persisted longer and the recession was markedly slower. Due to the high hydraulic conductivity of the UCB and the 3:1 slope, we expected water tables to be short-lived (as Well W9.5 showed), and we suspect that effects from well installation, including smearing of walls and clogging of the screens, may have influenced the measurements. Lag times between the development of perched water tables within the UCB and the response at the trench were between 1 and 2 h. The drainage of the hillslope persisted for many days following the cessation of storm rainfall, likely sustained by vertical drainage of the GM into the UCB.

Reproducing Field Observations with an Uncalibrated Model

We used the series of rain events in July 2007 to test our initial parameterization of the model (Fig. 9). Simulated lag times between peak rainfall and peak discharge were on the order of 3 to 8 h, which was only slightly longer than observed in the field. The overall subsurface runoff coefficient in the model for the July 2007 rain storms was 61%, which agrees very well with the subsurface runoff coefficient of 62% observed in the field. Subsurface runoff coefficients for the individual storm events were 9 to 71%. Actual evapotranspiration accounted for 21% of the input, and actual evapotranspiration was equal to potential evapotranspiration, indicating that this site is not moisture-limited. No surface runoff occurred, which matched field observations. In the model, subsurface flow only left the model domain through the UCB, as opposed to field observations with ~15% of the subsurface flow coming from the GM. As mentioned above, the geofabric was not represented in the model, but field

observations indicated it provided a preferred pathway for outflow from the GM. Although peak flows were often underestimated and baseflow sometimes overestimated, the agreement between field-measured and simulated total lateral subsurface flow was surprisingly good, especially with regard to timing and slopes of

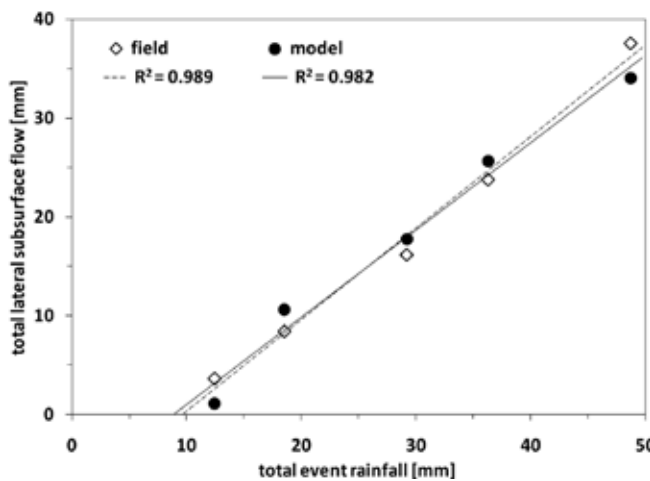


Fig. 7. Linear relation between event size and measured or simulated total lateral subsurface flow. The x axis intercept of trend lines indicates a precipitation threshold of 9.7 mm for field observations and 8.9 mm for simulated hydrologic response.

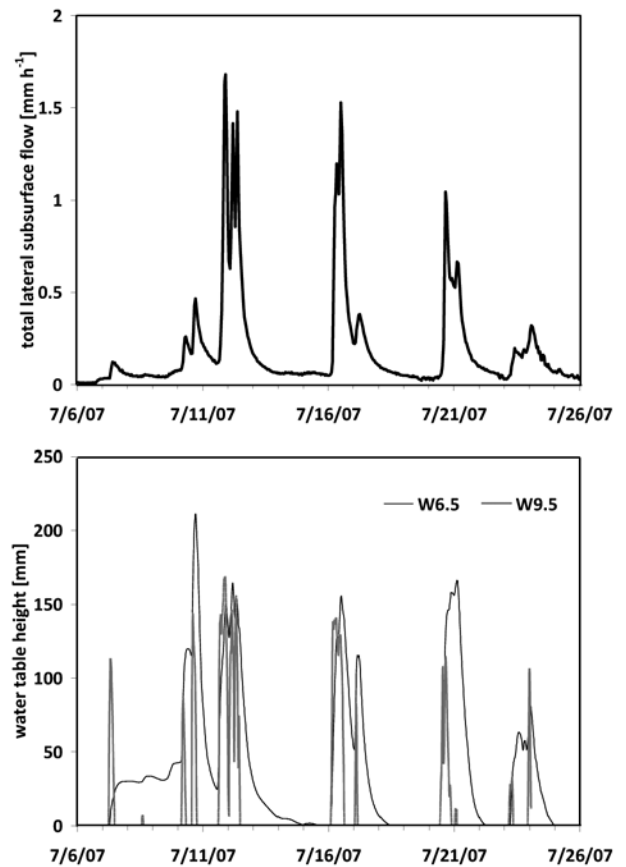


Fig. 8. Observed total lateral subsurface flow (top) and water table heights at the upper capillary break–barrier layer interface, measured in the two wells (bottom), in response to July 2007 rain events.

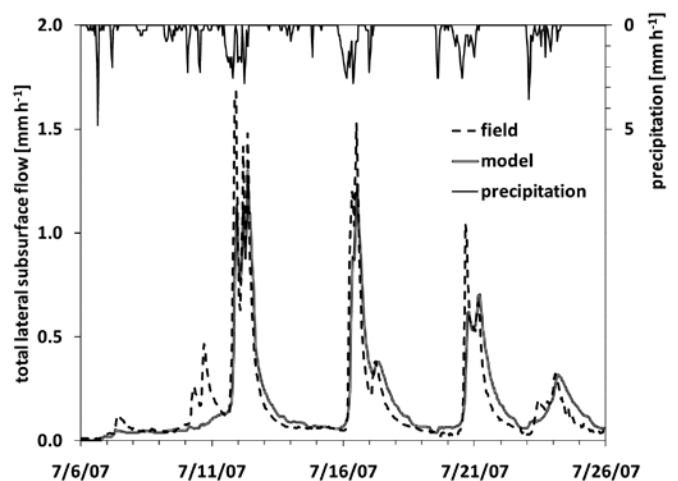


Fig. 9. Comparison between measured and simulated lateral subsurface flow for the July 2007 rain events.

rising and falling limbs of the simulated hydrographs. This was particularly encouraging because model parameters were not adjusted and were based solely on actual measurements; that is, this model was uncalibrated. The Nash–Sutcliffe efficiency statistic for the log-transformed values of total discharge was 0.73, indicating a high degree of agreement between field data and model. The relationship between total event rainfall and total lateral subsurface flow for the five storm events was very similar to field data, with a calculated precipitation threshold for the initiation of lateral subsurface flow of approximately 9 mm (Fig. 7).

Internal Flow Process Examination and Water Balance Estimation

While direct examination of internal flow processes within the cover was impossible (beyond the trench construction and limited well placement), we examined these processes with tracer experiments associated with the sprinkling experiment and with the model. The tracer breakthrough curve showed a fast rise in concentrations and a long tailing (Fig. 10). Six hours after the tracer injection lateral subsurface flow had dropped significantly (Fig. 5) and mass fluxes of tracer were small. The concentration peaked 2.25 h after the injection. The estimated mean lateral subsurface flow velocity was 4.2 m h⁻¹, indicating fast lateral flow under very wet conditions. Twenty-four percent of the total applied tracer mass was recovered within 7 h after injection. The loss of the tracer can be accounted for by alternative flowpaths that were not captured at the trench face, the potential for residual tracer held in the UCB that was released over a long period of time, and loss of tracer into the BL.

Internal flow processes were also explored with the model by simulating the hydrologic response to climatic data of 2006 (Fig. 11). Total lateral subsurface flow accounted for approximately 68% of the total rainfall (Fig. 12). Actual evapotranspiration was 17% (2% evaporation, 15% transpiration) and equaled potential evapotranspiration. The simulation indicated that 15% of the input left the upper part of the cover system (GM, UCB, and BL) as vertical percolation from the bottom of the BL. The relative saturation of the individual layers of the cover system throughout the year indicated that the GM almost always remained above 80% of saturation (Fig. 13). The moisture in this layer was influenced by precipitation as well as evapotranspiration fluxes. The UCB material does not have a high water retention capacity, and therefore mostly had low water contents, reflecting the precipitation dynamics closely. The BL remained practically saturated the entire year. The LCB did not show any pronounced variability in relative saturation over the year, suggesting that it is well buffered from near-surface dynamics. The model showed no development of positive pressure heads in the GM.

It was interesting to note that despite the common assumption of predominantly vertical flow in the unsaturated zone the flow trajectories of the particles released in the GM within the model showed a pronounced lateral flow component (Fig. 14). Between events, during drainage of the cover, a more slope-parallel hydraulic

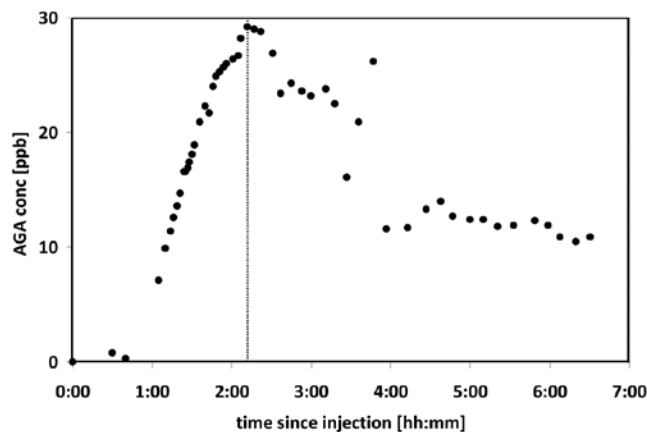


Fig. 10. Amino G acid tracer breakthrough curve measured in composite total lateral subsurface flow from the growth medium and upper capillary break. Dashed line indicates time of peak tracer concentration.

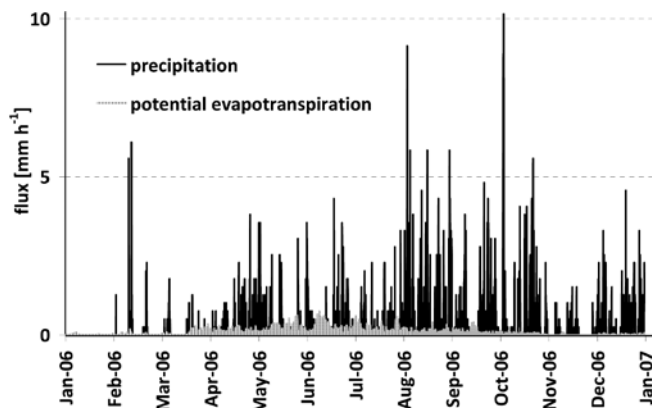


Fig. 11. Measured precipitation and estimated potential evapotranspiration determined from 2006 onsite meteorological data.

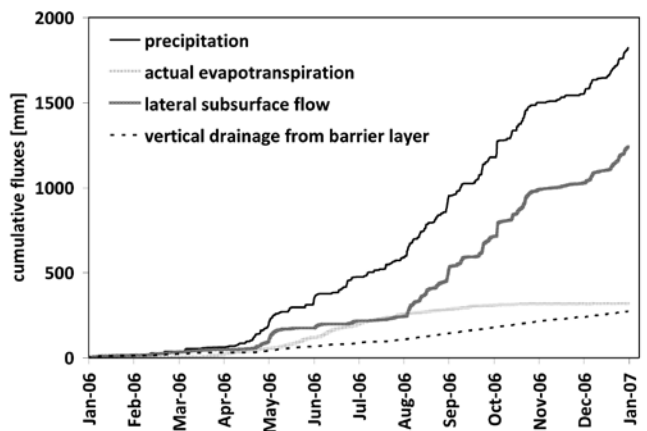


Fig. 12. Simulated water balance of the cover system for 2006.

gradient developed driving flow laterally downslope within the GM. Also a capillary barrier effect between the finer grained GM and the very coarse UCB during drier periods resulted in flow vectors being oriented parallel to the layer interface. During the

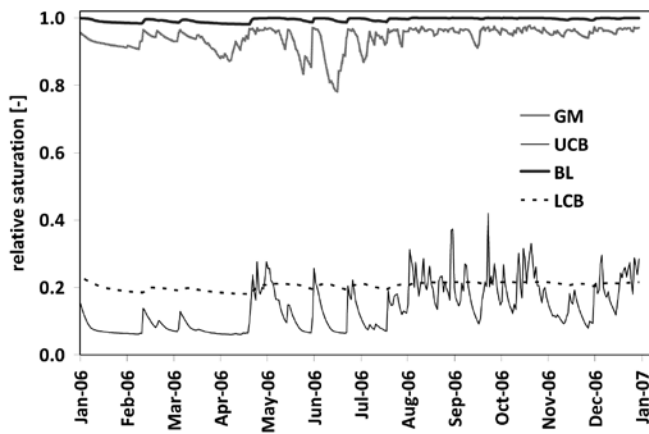


Fig. 13. Soil water storage expressed as simulated relative saturation for the four cover layers (GM, growth medium; UCB/LCB, upper/lower capillary break; BL, barrier layer).

frequent events, however, vertical flow in the GM dominated with water flowing from the GM into the UCB. The particle released at location A in the GM flowed into the UCB during a 55-mm storm in early May and reached the trench face 24 h later. The particle released in the GM at location B, however, did not reach the trench face. It entered the UCB during the same storm in early May as the particle released in the GM in location A. During this storm and the recession of lateral subsurface flow in the UCB, it moved

downslope along the interface between UCB and BL toward the trench. As soon as lateral subsurface flow subsided the particle was diverted to vertical downward flow and entered the BL in mid May, during a period of less intense and less frequent rainfalls, higher potential evapotranspiration and decreasing soil moisture in the GM (Fig. 11–13). The particles released at both the A and B locations in the BL were subject only to vertical flow and ultimately flowed through the BL and LCB into the waste rock.

Discussion

One of the performance goals of cover systems in humid environments is to generate as much lateral subsurface flow within the cover as possible to minimize the vertical flow through the cover into the underlying waste material. Cover system behavior and performance in these environments, however, is still not well understood. Here, our trench-based approach has contributed to a better understanding of cover system performance and internal cover dynamics. Our uncalibrated model was able to represent well the measured lateral flow dynamics.

Internal Moisture Dynamics of the Cover System

In the context of model testing, the measured lateral flow was a useful variable and instrumental in increasing the confidence in the model parameterization. The partitioning of 2006 rainfall simulated by the model corresponded well with

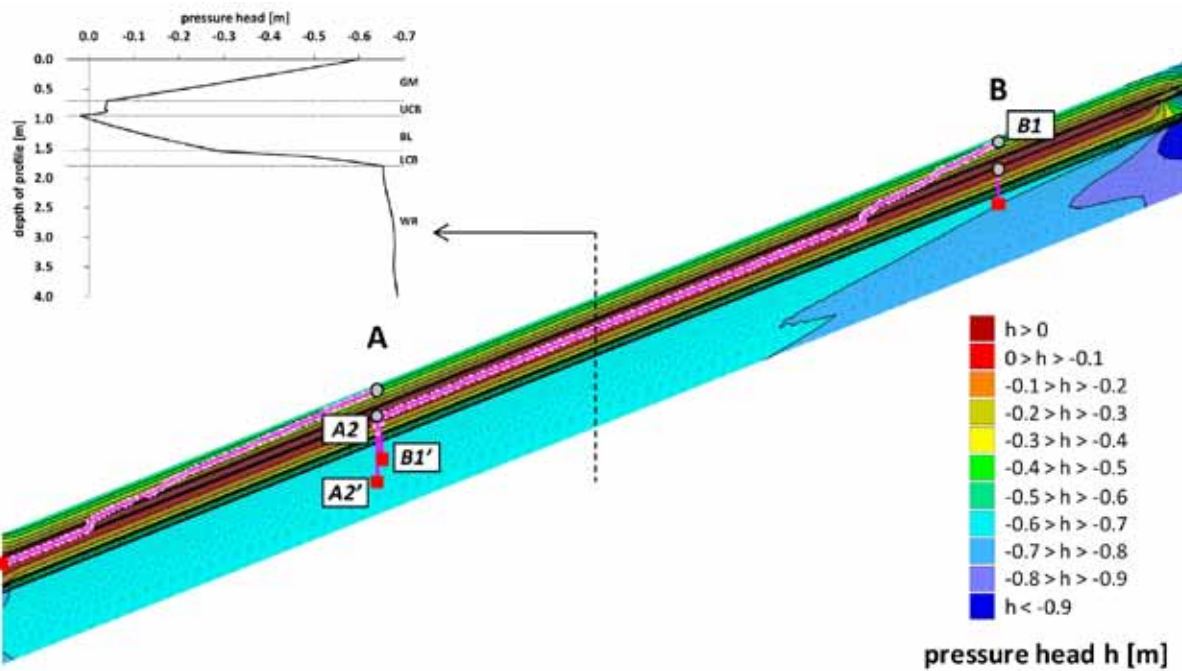


Fig. 14. Pressure head distribution in the cover system at the end of the 1-yr simulation and trajectories of flowing particles (shown in pink) during the 1-yr simulation. Dashed line shows location of cross-section for which the pressure head profile is shown (GM, growth medium; UCB/LCB, upper/lower capillary break; BL, barrier layer; WR, waste rock). Flowing particles were released in the GM and in the BL at the midslope (A) and upslope (B) location at the start of the simulation. Gray dots show initial location of flowing particles; red squares are final location at the end of the simulation. For clarification, A2–A2' is trajectory of particle released in BL midslope, and B1–B1' is the trajectory of particle released in GM upslope.

water balance estimates based on field measurements of climate and the lysimeter monitoring results (Table 2). Lysimeter measurements and model simulation showed the same range of vertical percolation below the BL, suggesting that the lysimeter does not overestimate vertical net percolation to a large extent. The model helped us to better understand the internal flow behavior of the BL.

The simulated pressure head profile that developed within the BL showed a downward vertical gradient (Fig. 14). Since the BL is nearly saturated the entire time, water can travel at near-maximum pore-water velocities through the saturated BL. The plot of the relative saturation (Fig. 13) shows that the design criterion of maintaining at least 85% saturation in the BL is met. Therefore oxygen diffusion into the waste rock is minimized. The requirement to maintain saturation in the BL makes the development of the vertical pressure head gradient inevitable. The saturated conductivity contrast between waste rock and LCB is not sufficient to generate perched water tables and subsequent lateral flow. It is therefore reasonable to assume that the water flux across the bottom of the BL will enter the waste rock. Reducing BL saturated conductivity via either greater compaction or reducing material grain size would limit water flux through the BL and increase flow in the UCB. Recent studies of the post-construction evolution of cover systems (Benson et al., 2007) suggest that saturated hydraulic conductivities of some cover materials increase over time due to development of structure (macropores) and heterogeneity. Therefore, it is important to select materials with grain size distributions that are less prone to the development of cracks and to maximize compaction of the BL during cover construction. However, the long-term conservation of the specifications of barrier layers remains a challenge.

The water balance modeling further showed that no positive pressure heads occurred in the GM. This indicated that transient perched water tables that develop in the UCB most likely do not rise into the GM. Minimizing buildup of head in the GM improves long-term stability of the cover.

The discrepancy between subsurface fluxes from the GM and UCB in the field relative to the model is of interest. We did not represent the layer of geofabric in the model (as explained above), and the model did not simulate pressure heads exceeding zero for the GM exposure at the trench face during the modeled period, resulting in no simulated outflow from this layer owing to the prescribed seepage-face boundary condition. We therefore hypothesize that the lateral outflow from the GM that was observed in the field was due to the presence of the geofabric (placed between GM and UCB). It remains unclear at this point, however, if the root mat that has developed on top of the geofabric since construction leads to this behavior, or at least contributes to it.

Table 2. Comparison between water balance estimates based on field data and water balance simulation for meteorological data of 2006.

	Field data†		Model	
	mm	%	mm	%
Precipitation	1941‡	100	1822	100
Lateral subsurface flow	1326§	68	1240	68
Actual evapotranspiration	251	13	319	17
Change in storage	0	–	~0	–
Vertical percolation into waste rock	363	19	274	15¶

† Field data were taken from the 2006 cover performance monitoring report compiled by O’Kane Consultants (Saskatoon, SK, Canada) and provided by Hecla Greens Creek Mining Company.

‡ Includes total snowmelt. However, hourly precipitation data including snowmelt were not available; therefore, only rainfall precipitation was used in the model input.

§ Calculated as difference between precipitation, estimated actual evapotranspiration, and measured vertical percolation into waste rock (lysimeter).

¶ Quantified as flux across the bottom of the barrier layer.

Hydrologic Behavior and Performance of the Cover—Comparison with Natural Analogs

While many studies have tested the performance of installed covers by monitoring moisture conditions over a few years (O’Kane et al., 1998; Hockley et al., 2003; Weeks and Wilson, 2005; Adu-Wusu and Yanful, 2006), to our knowledge our work is the first to measure lateral flow from different depths directly and to use lateral flow as a diagnostic for internal cover performance. The physics-based model that we used, HYDRUS-2D, was able to reproduce satisfactorily the total lateral subsurface flow without calibration. This reflects the highly engineered nature of the system whose materials were well characterized during design and construction. Such calibration-free successes are rare on natural hillslopes where soil and topographic heterogeneity hamper the application of physics-based approaches in an uncalibrated mode (Ebel et al., 2008). Clearly cover systems themselves evolve as they are exposed to environmental conditions and develop heterogeneity over some number of years following construction, resulting in a change of hydraulic properties of the soil materials and, thus, the hydrologic response (Breshears et al., 2005; Benson et al., 2007; Suter et al., 1993). Breshears et al. (2005) argued that with time the influence of the engineering process on cover behavior decreases, and environmental processes increasingly shape the performance (see their Fig. 7). After almost a decade in service, the cover system presented here still seems to exhibit the original hydraulic characteristics, as indicated by the fact that an uncalibrated model using hydraulic parameters determined 7 to 10 yr ago during cover design and construction was able to describe the hydrological behavior of the cover.

While no long-term data exist on the evolution of engineered covers, it can be expected that as the cover system evolves and heterogeneity develops through the years this uncalibrated model using parameters from the time of or shortly after construction will eventually not be able to describe water flow in the cover system

adequately. Understanding the evolution of hydrologic systems and interactions with biota remains one of the big challenges in hydrology, and efforts are currently underway elsewhere to investigate the co-evolution of a coupled hydrology–vegetation system at the hillslope scale (Hopp et al., 2009).

Studies have called for cover system designs that accommodate environmental processes rather than resist them (Clarke et al., 2004). The question may then be asked: how does an engineered cover compare to a natural hillslope? Our trench approach used in this study is a well-grounded methodology in hillslope hydrology and has been used at the base of hillsides at numerous sites around the world for several decades (see early work by Whipkey, 1965; Dunne and Black, 1970; Mosley, 1979; McDonnell, 1990). The generation of lateral subsurface flow within the cover seemed to be equivalent to flow generated along a soil–bedrock interface. This type of subsurface flow has been found in other steep and humid environments where shallow soils are underlain by much less permeable bedrock, for example, the H.J. Andrews Experimental Forest, Oregon, USA (McGuire et al., 2007); the Maimai catchment in New Zealand (McGlynn et al., 2002); the Panola experimental hillslope in Georgia, USA (Freer et al., 2002; Tromp-van Meerveld and McDonnell, 2006); and the Canadian Shield region in Ontario, Canada (Buttle and Turcotte, 1999). Transient perched water tables typically develop at the soil–bedrock interface as response to storm input, leading to fast saturated (or near-saturated) lateral subsurface flow. Such transient water table development on steep, responsive natural hillslopes is also quite flashy. McDonnell (1990) reported water table longevity following rainfall on the order of 12 h or less. Often preferential flow features like soil pipes or gaps have developed at the interface to accommodate subsurface stormflow. Our well data indicated the occurrence of short-lived water tables perching at the interface of UCB and BL. The UCB layer acted as the main flow path, delivering the majority of subsurface flow at the trench.

Our measured response to the July 2007 rain events revealed a flashy response behavior of the cover where individual rain events generated distinct trench responses. Flashy responses have been attributed to the presence of threshold processes (nonlinear behavior) that require the exceedance of moisture storage capacity before fast flow is generated. In our case, a threshold is generated by the slight capillary barrier effect between the finer-grained GM and the very coarse UCB that increases the storage capacity of the GM by $\sim 2\%$ (v/v) beyond its field capacity. Our estimated overall rainfall threshold for inducing measurable lateral flow was 10 mm. This is at the extreme lower end of rainfall thresholds for natural slopes reported in the literature (Weiler et al., 2005). For instance, McDonnell (1990) reported values on the order of 20 mm at the Maimai experimental hillslope in New Zealand to 30 mm at the H.J. Andrews Experimental Forest in Oregon, USA (McGuire, 2004) to 55 mm at the Panola hillslope in Georgia,

USA (Tromp-van Meerveld and McDonnell, 2006), and more than 80 mm of rainfall at the Savannah River Site in South Carolina (Hopp et al., 2010, unpublished data).

In terms of subsurface runoff coefficients, our slope again is at the high efficiency end of the spectrum, where for the July events, this value ranged from 29 to 77%. These values are more than double the values from natural hillslope analogs, as reviewed in Weiler et al. (2005). In view of cover performance the low precipitation threshold for the initiation of lateral subsurface flow and the high subsurface runoff coefficients achieved are desirable and point to a high efficiency of the cover system. It is difficult to predict the trajectory of drainability of our site. One might expect the very flashy and responsive lateral subsurface flow regime to move to a less flashy behavior as the system changes due to ecohydrological interactions and hydrogeological development. Nevertheless, natural systems appear generally to develop better and more efficient strategies over time to deal with the periodic high inputs (Bejan, 2007).

Conclusions

The performance of cover systems over mine waste rock has primarily been evaluated with regard to vertical net percolation through the cover. In humid, temperate environments (with annual precipitation $>$ annual potential evapotranspiration) one option to minimize vertical net percolation into underlying waste rock is to design covers such that they divert infiltrating precipitation to lateral subsurface flow downslope within the cover. However, this component of the water balance of a cover is rarely measured directly. To our knowledge, our study is the first to trench and monitor a complex multilayered test cover in high temporal resolution. The cover design was very responsive to precipitation, converting approximately two-thirds of the input to lateral subsurface flow. Compared to natural hillslope sites, this indicates an efficient generation of subsurface flow. Lateral subsurface flow is preceded by the development of transient perched water tables at the interface of the coarse capillary break and compacted barrier layer. We parameterized a finite element model based on measured and estimated material properties without performing any calibration. Our model was able to reproduce field observations of total lateral subsurface flow measured at the trench. Model results confirmed field lysimeter measurements of vertical net percolation and helped to better understand the water balance and internal flow behavior of the cover. Our water balance simulations indicated that flow through the barrier layer is driven by a small but permanent vertical pressure head gradient that develops within the barrier layer and results in vertical net percolation of approximately 15% of the input. Reducing the saturated hydraulic conductivity of the barrier layer, for example, by selecting a finer grained material or by augmenting the current material, may be an option to further decrease flow through the cover.

Acknowledgments

The authors gratefully acknowledge the assistance of Adam Mazurkiewicz, Daniele Penna, and Frauke Barthold in installing and operating the field equipment. Discussions with O'Kane Consultants, Saskatoon, Saskatchewan, Canada provided helpful insight and valuable information. We also thank three anonymous reviewers and the associate editor for constructive feedback. This research was funded by Hecla Greens Creek Mining Company.

References

- Adu-Wusu, C., and E.K. Yanful. 2006. Performance of engineered test covers on acid-generating waste rock at Whistle mine, Ontario. *Can. Geotech. J.* 43:1–18.
- Albright, W.H., C.H. Benson, G.W. Gee, A.C. Roesler, T. Abichou, P. Apiwantragoon, B.F. Lyles, and S.A. Rock. 2004. Field water balance of landfill final covers. *J. Environ. Qual.* 33:2317–2332.
- Allen, R.G., M.E. Jensen, J.L. Wright, and R.D. Burman. 1989. Operational estimates of reference evapotranspiration. *Agron. J.* 81:650–662.
- Ayres, B., G. Dirom, D. Christensen, S. Januszewski, and M. O'Kane. 2003. Performance of cover system field trials for waste rock at Myra Falls Operations. p. 1195. *In* 6th International Conference on Acid Rock Drainage, Cairns, Australia. 14–17 July 2003. The Australasian Institute of Mining and Metallurgy, Carlton South, VIC, Australia.
- Bejan, A. 2007. Constructal theory of pattern formation. *Hydrol. Earth Syst. Sci.* 11:753–768.
- Benson, C., T. Abichou, W. Albright, G. Gee, and A. Roesler. 2001. Field evaluation of alternative earthen final covers. *Int. J. Phytoremed.* 3:105–127.
- Benson, C.H., A. Sawangsurriya, B. Trzebiatowski, and W.H. Albright. 2007. Postconstruction changes in the hydraulic properties of water balance cover soils. *J. Geotech. Geoenviron. Eng.* 133:349–359.
- Bews, B.E., S.L. Barbour, and B. Wickland. 1999. Lysimeter design in theory and practice. p. 13–21. *In* Sixth International Conference on Tailings and Mine Waste '99, Fort Collins, Colorado. 24–27 Jan. 1999. A.A. Balkema, Rotterdam.
- Bohnhoff, G.L., A.S. Ogorzalek, C.H. Benson, C.D. Shackelford, and P. Apiwantragoon. 2009. Field data and water-balance predictions for a monolithic cover in a semiarid climate. *J. Geotech. Geoenviron. Eng.* 135:333–348.
- Bouazza, A., J.G. Zornberg, J.S. McCartney, and H. Nahlawi. 2006. Significance of unsaturated behaviour of geotextiles in earthen structures. *Aust. Geomech.* 41:133–142.
- Breshears, D.D., J.W. Nyhan, and D.W. Davenport. 2005. Ecohydrology monitoring and excavation of semiarid landfill covers a decade after installation. *Vadose Zone J.* 4:798–810.
- Buttle, J.M., and D.S. Turcotte. 1999. Runoff processes on a forested slope on the Canadian shield. *Nord. Hydrol.* 30:1–20.
- Clarke, J.H., M.M. MacDonell, E.D. Smith, R.J. Dunn, and W.J. Waugh. 2004. Engineered containment and control systems: Nurturing nature. *Risk Anal.* 24:771–779.
- Dunne, T., and R.D. Black. 1970. Partial area contributions to storm runoff in a small New England watershed. *Water Resour. Res.* 6:1296–1311.
- Dwyer, S.F. 2003. Water balance measurements and computer simulations of landfill covers. Ph.D. diss. Univ. of New Mexico, Albuquerque.
- Ebel, B.A., K. Loague, D.R. Montgomery, and W.E. Dietrich. 2008. Physics-based continuous simulation of long-term near-surface hydrologic response for the Coos Bay experimental catchment. *Water Resour. Res.* 44:W07417, doi:10.1029/2007WR006442.
- Feddes, R.A., P.J. Kowalik, and H. Zaradny. 1978. Simulation of field water use and crop yield. Simulation Monographs. Pudoc, Center for Agricultural Publishing and Documentation, Wageningen, the Netherlands.
- Freer, J., J.J. McDonnell, K.J. Beven, N.E. Peters, D.A. Burns, R.P. Hooper, B. Aulenbach, and C. Kendall. 2002. The role of bedrock topography on subsurface storm flow. *Water Resour. Res.* 38:1269, doi:10.1029/2001WR000872.
- Hockley, D.E., M. Noel, E.M. Rykaart, S. Hahn, and M. Paul. 2003. Testing of soil covers for waste rock in the Ronneburg WISMUT mine closure. p. 1195. *In* 6th International Conference on Acid Rock Drainage, Cairns, Australia. 14–17 July 2003. The Australasian Institute of Mining and Metallurgy, Carlton South, VIC, Australia.
- Hopp, L., C. Harman, S. Desilets, C. Graham, J. McDonnell, and P. Troch. 2009. Hillslope hydrology under glass: Confronting fundamental questions of soil-water-biota co-evolution at Biosphere 2. *Hydrol. Earth Syst. Sci. Disc.* 6:4411–4448.
- Iryo, T., and R.K. Rowe. 2003. On the hydraulic behavior of unsaturated nonwoven geotextiles. *Geotext. Geomembranes* 21:381–404.
- Kelln, C., L. Barbour, and C. Qualizza. 2007. Preferential flow in a reclamation cover: Hydrological and geochemical response. *J. Geotech. Geoenviron. Eng.* 133:1277–1289.
- Kelln, C.J., S.L. Barbour, and C. Qualizza. 2009. Fracture-dominated subsurface flow and transport in a sloping reclamation cover. *Vadose Zone J.* 8:96–107.
- Krause, P., D.P. Boyle, and F. Bäse. 2005. Comparison of different efficiency criteria for hydrological model assessment. *Adv. Geosci.* 5:89–97.
- McDonnell, J.J. 1990. A rationale for old water discharge through macropores in a steep, humid catchment. *Water Resour. Res.* 26:2821–2832.
- McGlynn, B.L., J.J. McDonnell, and D.D. Brammer. 2002. A review of the evolving perceptual model of hillslope flowpaths at the Maimai catchments, New Zealand. *J. Hydrol.* 257:1–26.
- McGuire, K.J. 2004. Water residence time and runoff generation in the Western Cascades of Oregon. Ph.D. diss. Dep. of Forest Engineering, Oregon State University, Corvallis.
- McGuire, K.J., M. Weiler, and J.J. McDonnell. 2007. Integrating tracer experiments with modeling to assess runoff processes and water transit times. *Adv. Water Resour.* 30:824–837.
- McGuire, P.E., B.J. Andraski, and R.E. Archibald. 2009. Case study of a full-scale evapotranspiration cover. *J. Geotech. Geoenviron. Eng.* 135:316–332.
- Monteith, J.L. 1981. Evaporation and surface temperature. *Q. J. R. Meteorol. Soc.* 107:1–27.
- Monteith, J.L., and M.H. Unsworth. 1990. Principles of environmental physics. Edward Arnold, London.
- Morris, C.E., and J.C. Stormont. 1999. Parametric study of unsaturated drainage layers in a capillary barrier. *J. Geotech. Geoenviron. Eng.* 125:1057–1065.
- Mosley, M.P. 1979. Streamflow generation in a forested watershed, New Zealand. *Water Resour. Res.* 15:795–806.
- Nahlawi, H., A. Bouazza, and J. Kodikara. 2007. Characterisation of geotextiles water retention using a modified capillary pressure cell. *Geotextiles Geomembranes* 25:186–193.
- Nash, J.E., and J.V. Sutcliffe. 1970. River flow forecasting through conceptual models part I—A discussion of principles. *J. Hydrol.* 10:282–290.
- Nyhan, J.W. 2005. A seven-year water balance study of an evapotranspiration landfill cover varying in slope for semiarid regions. *Vadose Zone J.* 4:466–480.
- O'Kane, M. 1996. Instrumentation and monitoring of an engineered soil cover for acid generating mine waste. M.Sc. thesis. Dep. of Civil Engineering, University of Saskatchewan, Saskatoon.
- O'Kane, M., G.W. Wilson, and S.L. Barbour. 1998. Instrumentation and monitoring of an engineered soil cover system for mine waste rock. *Can. Geotech. J.* 35:828–846.
- Penman, H.L. 1948. Natural evaporation from open water, bare soil and grass. *Proc. R. Soc. A* 193:120–145.
- Simms, P.H., and E.K. Yanful. 1999. Some insights into the performance of an experimental soil cover near London, Ontario. *Can. Geotech. J.* 36:846–860.
- Simunek, J., M.T. van Genuchten, and M. Sejna. 2006. The HYDRUS software package for simulating two- and three-dimensional movement of water, heat, and multiple solutes in variably-saturated media: Technical manual. Version 1.0. PC-Progress, Prague, Czech Republic.
- Sinclair, T.R. 2006. A reminder of the limitations in using Beer's Law to estimate daily radiation interception by vegetation. *Crop Sci.* 46:2343–2347.
- Stormont, J.C., K.S. Henry, and T.M. Evans. 1997. Water retention functions of four nonwoven polypropylene geotextiles. *Geosynth. Int.* 4:661–672.
- Suter, G.W. II, R.J. Luxmoore, and E.D. Smith. 1993. Compacted soil barriers at abandoned landfill sites are likely to fail in the long term. *J. Environ. Qual.* 22:217–226.
- Tromp-van Meerveld, H.J., and J.J. McDonnell. 2006. Threshold relations in subsurface stormflow: 1. A 147-storm analysis of the Panola hillslope. *Water Resour. Res.* 42:W02410, doi:10.1029/2004WR003778.
- van Genuchten, M.Th. 1980. A closed-form equation for predicting the hydraulic conductivity of unsaturated soils. *Soil Sci. Soc. Am. J.* 44:892–898.
- Ward, A.L., and G.W. Gee. 1997. Performance evaluation of a field-scale surface barrier. *J. Environ. Qual.* 26:694–705.
- Weeks, B., and G.W. Wilson. 2005. Variations in moisture content for a soil cover over a 10 year period. *Can. Geotech. J.* 42:1615–1630.
- Weiler, M., J.J. McDonnell, H.J. Tromp-van Meerveld, and T. Uchida. 2005. Subsurface stormflow runoff generation processes. p. 1719–1732. *In* Encyclopedia of hydrological sciences. Wiley, New York.
- Whipkey, R.Z. 1965. Subsurface stormflow from forested slopes. *Bull. Int. Assoc. Sci. Hydrol.* 10:74–85.
- Yanful, E.K., P.H. Simms, R.K. Rowe, and G. Stratford. 1999. Monitoring an experimental soil water cover near London, Ontario, Canada. *Geotech. Geol. Eng.* 17:65–84.